

Ruthenium and Rhenium Complexes of Fluorene-Based Bipyridine Ligands: Synthesis, Spectra, and Electrochemistry

K. R. Justin Thomas,[†] Jiann T. Lin,^{*,†} Hsiu-Mei Lin,[†] Chen-Pin Chang,[‡] and Chang-Hao Chuen[‡]

*Institute of Chemistry, Academia Sinica, Taipei, Taiwan 115, Republic of China, and
Department of Chemistry, Fu-Jen Catholic University,
Hsinchuang, Taipei 242, Taiwan, Republic of China*

Received September 5, 2000

Bipyridine ligands featuring fluorene and ferrocene in the conjugation chain were synthesized by Pd(II)/Cu(I)-catalyzed Sonogashira coupling reactions, and their complexation behavior was investigated. The octahedral complexes formed by refluxing Ru(bpy)₂Cl₂ and Re(CO)₅Cl with the ligands in ethanol or benzene were characterized by NMR, electronic spectra, fluorescence spectra, mass spectra, elemental analyses, and electrochemical studies. The bipyridine ligands and the complexes except the ferrocene-containing compounds are luminescent at room temperature. The luminescence in the ruthenium complexes is possibly from a MLCT state, and the fluorescence due to the ligand is completely quenched. When compared to the Ru(bpy)₃²⁺, the ruthenium complexes studied in this work exhibit longer lifetimes, which probably stems from the delocalization of charge into the extended fluorene conjugation. The crystal structure of a ferrocenyl fluorene derivative is also reported.

Introduction

Ruthenium polypyridyl complexes continue to attract wide attention owing to their applications in molecular devices based on photoinduced electron and energy transfer reactions^{1–3} and in the fabrication of organic light-emitting diodes.^{4–6} Since the luminescence in these complexes are from a metal-to-ligand charge transfer (MLCT) state it is possible to tune the excited state properties such as luminescence wavelength, lifetime, and quantum yield by tailoring the ligand features and structure and rigidity of the complexes.^{7–9} Numerous studies correlated well the dependence of absorption and

luminescence properties to the energy levels of low lying states, electron delocalization on the acceptor ligand, and structure and rigidity. Polypyridyl ligands with extended polyaromatic conjugation have been found to exhibit prolonged excited states. In this context, benzene-, anthracene-, and pyrene-containing polypyridyl complexes were studied with promising outcome.^{10–12}

Recently, fluorene is increasingly used as a constituent in materials used for electrooptic applications due to their strong luminescence, charge delocalization, and stability.^{13,14} However, to the best of our knowledge polypyridyl ligands incorporating fluorene in the conjugation are not yet reported.¹⁵ So, we set out a project to synthesize novel fluorene-containing ligands and

* Corresponding author. Fax: Int. code + (886)-(2) 27831237. E-mail: jtlin@chem.sinica.edu.tw.

[†] Academia Sinica.

[‡] Fu-Jen Catholic University.

(1) Bruce, D. W.; O'Hare, D., Eds. *Inorganic Materials*; John Wiley & Sons Ltd: Chichester, England, 1992.

(2) Wasielewski, M. R.; Johnson, D. G.; Svec, W. A.; Kersey, K. M.; Cragg, D. E.; Minsek, D. W. In *Photochemical Energy Conversion*; Norris, J. R., Meisel, D., Eds.; Elsevier: New York, 1989; p 135.

(3) Balzani, V.; Candola, F., Eds. *Supramolecular Photochemistry*; Ellis Horwood: Chichester, 1991.

(4) Lyons, C. H.; Abbas, E. D.; Lee, J.-K.; Rubner, M. F. *J. Am. Chem. Soc.* **1998**, *120*, 12100.

(5) Wu, A.; Yoo, D.; Lee, J.-K.; Rubner, M. F. *J. Am. Chem. Soc.* **1999**, *121*, 4883. (b) Elliott, C. M.; Pichot, F.; Bloom, C. J.; Rider, L. S. *J. Am. Chem. Soc.* **1998**, *120*, 6781.

(6) Gao, F. G.; Bard, A. J. *J. Am. Chem. Soc.* **2000**, *122*, 7426. (b) Handy, E. S.; Pal, A. J.; Rubner, M. F. *J. Am. Chem. Soc.* **1999**, *121*, 3525.

(7) Balzani, V.; Juris, A.; Venturi, M.; Campagna, S.; Serroni, S. *Chem. Rev.* **1996**, *96*, 759. (b) Harriman, A.; Ziessel, R. *Chem. Commun.* **1996**, 1707.

(8) Hissler, M.; El-ghayoury, A.; Harriman, A.; Ziessel, R. *Angew. Chem., Int. Ed. Engl.* **1998**, *37*, 1717. (b) Grosshenny, V.; Harriman, A.; Romero, M.; Ziessel, R. *J. Phys. Chem.* **1996**, *100*, 17472.

(9) Dumauer, N. H.; Boussic, T. R.; Devenney, M. McCusker, J. K. *J. Am. Chem. Soc.* **1997**, *119*, 8253. (b) Treadway, J. A.; Loeb, B.; Lopey, R.; Anderson, P. A.; Keene, F. R.; Meyer, T. J. *Inorg. Chem.* **1996**, *35*, 2242.

(10) Ziessel, R.; Hissler, M.; El-ghayoury, A.; Harriman, A. *Coord. Chem. Rev.* **1998**, *178–180*, 1251. (b) Sauvage, J.-P.; Collin, J.-P.; Chambron, J.-C.; Guillerez, S. Coudret, C.; Balzani, V.; Barigelletti, F.; De Cola, L.; Flamigni, L. *Chem. Rev.* **1994**, *94*, 993.

(11) Albano, G.; Balzani, V.; Constable, E. C.; Maestri, M.; Smith, D. R. *Inorg. Chim. Acta* **1998**, *277*, 225. (b) Wilson, G. J.; Lavnikonis, A.; Sasse, W. H. F.; Mau, A. W.-H. *J. Phys. Chem. (A)* **1997**, *101*, 4860. (c) Wilson, G. J.; Sasse, W. H. G.; Mau, A. W.-H. *Chem. Phys. Lett.* **1996**, *250*, 583.

(12) Harriman, A.; Hissler, M.; Khatri, A.; Ziessel, R. *Chem. Commun.* **1999**, 735. (b) Simon, J. A.; Curry, S. L. Schmehl, R. H.; Schatz, T. R.; Piotrowiak, P.; Jin, X.; Thummel, R. P. *J. Am. Chem. Soc.* **1997**, *119*, 11012. (c) Ford, W. E.; Rodgers, M. A. J. *J. Phys. Chem.* **1992**, *96*, 2917.

(13) Belfields, K. D.; Hagan, D. J.; Van Stryland, E. W.; Schafer, K. J.; Negres, R. A. *Org. Lett.* **1999**, *1*, 1575. (b) Reinhardt, B. A.; Brott, L. L.; Clarson, S. J.; Dillard, A. G.; Bhatt, J. L.; Kannan, R.; Yuan, L.; He, G. S.; Prasad, P. N. *Chem. Mater.* **1998**, *10*, 1863.

(14) Yu, W.-L.; Huang, P.-W.; Haeger, A. J. *Adv. Mater.* **2000**, *12*, 828. (b) Perepichka, I. F.; Popov, A. G.; Orekhova, T. V.; Bryce, M. R.; Andrievskii, A. M.; Batsanov, A. S.; Howard, J. A. K.; Sokolov, N. I. *J. Org. Chem.* **2000**, *65*, 3053. (c) Lee, J.-I.; Klaerner, G.; Miller, R. D. *Chem. Mater.* **1999**, *11*, 1083.

(15) While this work was in progress, there appeared a report describing fluorene-conjugated pyridine ligands and their molybdenum complexes. Behrendt, A.; Couchman, S. M.; Jeffery, J. C.; McCleverty, J. A.; Ward, M. D. *J. Chem. Soc., Dalton Trans.* **1999**, 4349.

their complexes and study their absorption, luminescence, and electrochemical properties. Herein, we report the synthesis, spectra, and electrochemistry of ruthenium(II) complexes derived from bipyridine ligands linked to fluorene units through an extended conjugation. Additionally we have also designed a ligand comprising fluorene and ferrocene moieties in order to investigate the possibility of electronic communication between ferrocene and ruthenium fragments. Heterobimetallic complexes are considered important in the field of homogeneous catalysis for their cooperative action¹⁶ and magnetochemistry if they possess one or two paramagnetic components.¹⁷

Experimental Section

General Comments. Unless otherwise noted, all operations were carried out under a dry, oxygen-free nitrogen atmosphere. Reagent grade tetrahydrofuran (THF) was distilled under nitrogen from sodium benzophenone ketyl. Diethylamine was distilled from KOH and stored under nitrogen atmosphere. Bulk grade hexane and dichloromethane were used as received for column chromatography separations. *n*-Butyllithium (1.6 M in hexane) was obtained from Aldrich Chemical Co. Inc. 5-Bromo-2,2'-bipyridine, 5,5'-dibromo-2,2'-bipyridine, and 9,9-diethyl-2-ethynyl-9H-fluorene were obtained according to the reported methods.^{18,19} In Sonogashira reactions, addition of 2 equiv of triphenylphosphine with reference to Pd(PPh₃)₂Cl₂ was beneficial and avoided the formation of colloidal palladium side products and darkening of the reaction mixtures. The NMR spectra were recorded on a Bruker AC300 spectrometer. Optical electronic spectra were measured in dichloromethane using a Cary 50 Probe UV-visible spectrophotometer. Emission spectra were recorded by a Hitachi F-4500 fluorescence spectrometer. Lifetime studies were performed by an Edingburgh FL 900 photon-counting system with a hydrogen-filled flash lamp or a nitrogen lamp as the excitation source. The temporal resolution after deconvolution of the excitation pulse was 200 ps. The data were analyzed using a nonlinear least-squares fitting program with a deconvolution method reported previously.²⁰ Cyclic voltammetry experiments were performed with a BAS-100 electrochemical analyzer. All measurements were carried out at room temperature with a conventional three-electrode configuration consisting of platinum working and auxiliary electrodes and a nonaqueous Ag/AgNO₃ reference electrode. The solvent in all experiments was CH₂Cl₂, and the supporting electrolyte was 0.1 M tetrabutylammonium perchlorate. The *E*_{1/2} values were determined as 1/2(*E*_pa + *E*_pc), where *E*_pa and *E*_pc are the anodic and cathodic peak potentials, respectively. All potentials are reported relative to Ag/AgNO₃ and are not corrected for the junction potential. Fc⁺/Fc was measured to be +0.220 V relative to Ag/AgNO₃. Mass spectra were obtained from a VG70-250S mass spectrometer. Elemental analyses were performed on a Perkin-Elmer 2400 CHN analyzer.

5-(9,9-Diethyl-9H-fluoren-2-ylethynyl)-2,2'-bipyridine (Fbpy) (1). Diethylamine (50 mL) was added to a flask containing 9,9-diethyl-2-ethynyl-9H-fluorene (1.23 g, 5 mmol), Pd(PPh₃)₂Cl₂ (35 mg), cuprous iodide (5 mg), triphenyl phosphine (26 mg), and 5-bromo-2,2'-bipyridine (1.17 g, 5 mmol)

under N₂ atmosphere and heated to reflux for 12 h. The cooled pale yellow mixture was evaporated to dryness, the residue was suspended over H₂O and extracted with diethyl ether (3 × 40 mL), and the organic layer was dried over anhydrous MgSO₄ and evaporated to yield a crude compound. It was further purified by column chromatography over SiO₂ using dichloromethane/hexane (4:1) as an eluant to obtain a colorless solid (1.46 g, 73%). ¹H NMR (CD₂Cl₂, 300 MHz): δ 0.32 (t, 7.4 Hz, 6 H, CH₃), 2.08 (q, 7.4 Hz, 4 H, CH₂), 7.36–7.38 (m, 4 H), 7.56–7.59 (m, 2 H), 7.73–7.76 (m, 2 H), 7.85 (td, 8.2, 2.0 Hz, 1 H), 7.96 (dd, 8.2, 2.1 Hz, 1 H), 8.46 (d, 8.3 Hz, 2 H), 8.67 (d, 2.1 Hz, 1 H), 8.82 (d, 1.4 Hz, 1 H). MS (FAB+): *m/z* 401 (M⁺ + 1). Anal. Calcd for C₂₉H₂₄N₂: C, 86.97; H, 6.04; N, 6.99. Found: C, 87.07; H, 5.87; N, 6.78.

5,5'-Bis(9,9-diethyl-9H-fluoren-2-ylethynyl)-2,2'-bipyridine (FbpyF) (2). It was prepared as described for **1** using 5,5'-dibromo-2,2'-bipyridine instead of 5-bromo-2,2'-bipyridine. Yield: 75%. ¹H NMR (CD₂Cl₂, 300 MHz): δ 0.33 (t, 7.3 Hz, 12 H, CH₃), 2.07 (q, 7.4 Hz, 8 H, CH₂), 7.34–7.40 (m, 6 H), 7.56–7.60 (m, 4 H), 7.73–7.76 (m, 4 H), 7.99 (d, 8.1 Hz, 2H), 8.48 (d, 8.1 Hz, 2 H), 8.84 (s, 1 H). MS (FAB+): *m/z* 646 (M⁺ + 1). Anal. Calcd for C₄₈H₄₀N₂: C, 89.40; H, 6.25; N, 4.34. Found: C, 89.54; H, 6.12; N, 4.48.

(9-Ferrocenylmethylene-9H-fluoren-2-ylethynyl)trimethylsilane (3a) and 2-Ethynyl-9-ferrocenylmethylene-9H-fluorene (3b). 2-Trimethylsilylethynylfluorene (2.62 g, 10 mmol) was dissolved in 50 mL of tetrahydrofuran and cooled to -75 °C. One equivalent of freshly prepared lithium-*N,N*-diisopropylamine was added dropwise over 30 min. After stirring at that temperature for 1 h, ferrocene carboxaldehyde (2.14 g, 10 mmol) dissolved in 20 mL of tetrahydrofuran was added through a dropping funnel. Subsequently, the reaction mixture was brought to room temperature slowly and allowed to stir at ambient temperature overnight. The reaction was quenched with aqueous ammonium chloride solution and extracted with diethyl ether. The combined organic extract was dried over anhydrous MgSO₄ and evaporated to leave a red tar weighing ~4.1 g (90%). NMR spectroscopy revealed a mixture of cis and trans isomers of **3a**. Attempts to separate them at this stage were unsuccessful. So desilylation was performed by treating the crude material dissolved in a 1:1 methanol/dichloromethane mixture with sodium hydroxide at room temperature for 6 h. Evaporation of the volatiles left viscous red oil. It was purified by column chromatography over silica gel using hexane/dichloromethane mixtures as eluant. Yield: 3.2 g (81%). The *E/Z* ratio was found to be 3:1. Pure *E*-isomer (**3b**) was obtained by careful crystallization from hexanes. ¹H NMR (acetone-*d*₆, 300 MHz): δ 3.68 (s, 1 H), 4.29 (s, 5 H), 4.54 (t, 1.7 Hz, 2 H), 4.77 (t, 1.7 Hz, 2 H), 7.26 (td, 8.5, 1.5 Hz, 1 H), 7.37 (t, 8.5 Hz, 1 H), 7.49 (dd, 8.6 Hz, 1.4 Hz, 1 H), 7.81–7.88 (m, 3 H), 8.07 (s, 1 H), 8.20 (d, 8.3 Hz, 1 H). Anal. Calcd for C₂₆H₁₈Fe: C, 80.85; H, 4.70. Found: C, 80.72; H, 4.71.

(9-Ferrocenylmethylene-9H-fluoren-2-ylethynyl)-2,2'-bipyridine (FcFbpy) (3). It was obtained in 82% yield as described for **1** using 5-bromo-2,2'-bipyridine and **3b**. ¹H NMR (CD₂Cl₂, 300 MHz): δ 4.25 (s, 5 H), 4.53 (t, 1.7 Hz, 2 H), 4.77 (t, 1.7 Hz, 2 H), 7.25 (td, 8.0 Hz, 1.4 Hz, 1 H), 7.32–7.40 (m, 2 H), 7.57–7.61 (m, 2 H), 7.76–7.88 (m, 3 H), 8.01 (dd, 8.1, 1.5 Hz, 1 H), 8.04 (s, 1 H), 8.23 (d, 8.0 Hz, 1 H), 8.45–8.49 (m, 2 H), 8.68 (d, 4.2 Hz, 1 H), 8.86 (s, 1 H). MS (FAB+): *m/z* 541 (M⁺ + 1). Anal. Calcd for C₃₆H₂₃FeN₂: C, 80.16; H, 4.30; N, 5.19. Found: C, 80.21; H, 4.19; N, 5.43.

[Ru(bpy)₂(Fbpy)](PF₆)₂ (4). An ethanol solution (20 mL) of ligand Fbpy (**1**) (100 mg, 0.25 mmol) and Ru(bpy)₂Cl₂·2H₂O (130 mg, 0.25 mmol) was refluxed for 12 h. The resulting red solution was cooled, and a saturated aqueous solution of NH₄-PF₆ was added. A red precipitate formed immediately; it was filtered, washed successively with water (10 mL), ethanol (10 mL), and diethyl ether (20 mL), and finally dried in vacuo. It was further purified by recrystallization from acetone/diethyl

(16) Kragl, V.; Dreisbach, C. *Angew. Chem., Int. Ed. Engl.* **1996**, *35*, 642.

(17) Bergerat, P.; Blumel, J.; Fritz, M.; Miermeier, J.; Hudeczek, P.; Kahn, O.; Kohler, F. *Angew. Chem., Int. Ed. Engl.* **1992**, *31*, 1258. (b) Kollmar, C.; Couty, M.; Kahn, O. *J. Am. Chem. Soc.* **1991**, *113*, 7994.

(18) Romero, F. M.; Ziessel, R. *Tetrahedron Lett.* **1995**, *36*, 6471.

(19) Tsuie, B.; Reddiger, J. L.; Sotzing, G. A.; Soloducho, J.; Katrizky, A. R.; Reynolds, J. R. *J. Mater. Chem.* **1999**, *9*, 2189.

(20) O'Connor, D. V.; Phillips, D. *Time-Correlated Single Photon Counting*; Academic: New York, 1984.

ether. Yield: 0.20 g (72%). ^1H NMR (acetone- d_6 , 400 MHz): δ 0.23 (t, 7.4 Hz, 6 H, CH_3), 2.07 (q, 7.4 Hz, 4 H, CH_2), 7.39–7.49 (m, 5 H), 7.57–7.62 (m, 5 H), 7.82–7.86 (m, 2 H), 8.01–8.08 (m, 4 H), 8.18–8.25 (m, 7 H), 8.3 (dd, 8.1, 2.0 Hz, 1 H), 8.8–8.84 (m, 6 H). $^{13}\text{C}\{^1\text{H}\}$ (acetone- d_6 , 300 MHz): δ 8.6, 33.0, 57.0, 85.1, 98.3, 120.4, 120.8, 121.2, 123.9, 124.9, 125.3, 128.4, 128.7, 126.9, 128.1, 128.7, 128.9, 129.1, 131.9, 139.0, 140.7, 141.2, 144.2, 150.9, 151.0, 151.5, 152.7, 152.9, 153.0, 154.0, 156.9, 157.6, 158.0, 158.06, 158.1. Anal. Calcd for $\text{C}_{49}\text{H}_{40}\text{F}_{12}\text{N}_6\text{P}_2\text{Ru}$: C, 53.31; H, 3.65; N, 7.61. Found: C, 52.95; H, 3.89; N, 7.52.

[Ru(bpy) $_2$ (FbpyF)](PF $_6$) $_2$ (5). Red microcrystalline **5** was prepared from FbpyF (**2**) as described above in 88% yield. ^1H NMR (acetone- d_6 , 400 MHz): δ 0.23 (t, 7.4 Hz, 12 H), 2.06 (m, 8 H), 7.37–7.48 (m, 10 H), 7.61–7.64 (m, 4 H), 7.82–7.87 (m, 4 H), 8.07 (d, 5.7 Hz, 2 H), 8.19–8.25 (m, 8 H), 8.34 (dd, 8.6, 2.2 Hz, 2 H), 8.82–8.91 (m, 6 H). $^{13}\text{C}\{^1\text{H}\}$ (acetone- d_6 , 300 MHz): δ 8.5, 32.8, 56.7, 84.1, 99.9, 119.4, 120.2, 120.7, 123.5, 124.8, 125.0, 125.5, 126.8, 127.5, 128.6, 128.7, 131.5, 138.8, 138.9, 140.6, 140.7, 144.1, 150.7, 150.8, 151.6, 151.7, 152.8, 155.1, 157.0, 157.1. Anal. Calcd for $\text{C}_{68}\text{H}_{56}\text{F}_{12}\text{N}_6\text{P}_2\text{Ru}$: C, 60.58; H, 4.19; N, 6.23. Found: C, 60.87; H, 3.96; N, 6.14.

Re(CO) $_3$ Cl[Fbpy] (6). The ligand Fbpy (**1**) (100 mg, 0.25 mmol) and $\text{Re}(\text{CO})_5\text{Cl}$ (90.3 mg, 0.25 mmol) were heated together in toluene (20 mL) at 60 °C for 8 h. The yellow precipitate formed was filtered, washed with hexane, and dried in vacuo to yield 160 mg (90%) of yellow solid. ^1H NMR (CDCl_3 , 300 MHz): δ 0.33 (t, 7.4 Hz, 6 H), 2.08 (q, 7.4 Hz, 4 H), 7.30–7.37 (m, 3 H), 7.50–7.59 (m, 3 H), 7.70–7.76 (m, 2 H), 8.06–8.17 (m, 4 H), 9.06 (d, 5.1 Hz, 1 H), 9.17 (s, 1 H). IR (CH_2Cl_2 , cm^{-1}): 1899 (s), 1921 (s), 2024 (s), 2209 (w). Anal. Calcd for $\text{C}_{32}\text{H}_{24}\text{ClN}_2\text{O}_3\text{Re}$: C, 54.42; H, 3.43; N, 3.97. Found: C, 54.40; H, 3.23; N, 4.09.

Re(CO) $_3$ Cl[FbpyF] (7). It was obtained as a dark yellow powder, using the method described above for **6** using FbpyF. Yield: 81%. ^1H NMR (CDCl_3 , 300 MHz): δ 0.34 (m, 12 H), 2.06 (q, 7.4 Hz, 8 H), 7.35 (m, 6 H), 7.54–7.57 (m, 4 H), 7.71 (d, 8.1 Hz, 4 H), 8.10 (s, br, 4 H), 9.17 (s, 2 H). IR (CH_2Cl_2 , cm^{-1}): 1898 (s), 1921 (s), 2024 (s), 2207 (w). Anal. Calcd for $\text{C}_{51}\text{H}_{40}\text{ClN}_2\text{O}_3\text{Re}$: C, 64.44; H, 4.24; N, 2.95. Found: C, 64.51; H, 4.39; N, 2.82.

[Ru(bpy) $_2$ (FcFbpy)](PF $_6$) $_2$ (8). Red microcrystalline **8** was prepared analogously to **5** using FcFbpy. ^1H NMR (acetone- d_6 , 300 MHz): δ 4.29 (s, 5 H), 4.58 (t, 1.7 Hz, 2 H), 4.78 (t, 1.6 Hz, 2 H), 7.32 (t, 8.0 Hz, 1 H), 7.38–7.44 (m, 2 H), 7.56–7.63 (m, 5 H), 7.75 (s, 1 H), 7.88 (t, 7.9 Hz, 2 H), 8.01–8.07 (m, 4 H), 8.11 (d, 7.9 Hz, 1 H), 8.19–8.25 (m, 8 H), 8.3 (dd, 8.0, 1.4 Hz, 1 H), 8.80–8.88 (m, 6 H). Anal. Calcd for $\text{C}_{56}\text{H}_{40}\text{F}_{12}\text{FeN}_6\text{P}_2\text{Ru}$: C, 54.08; H, 3.24; N, 6.76. Found: C, 53.80; H, 3.19; N, 6.59.

Re(CO) $_3$ Cl(FcFbpy) (9). It was obtained as a dark red powder using the method described for **7** using FcFbpy. ^1H NMR (CD_2Cl_2 , 300 MHz): δ 4.26 (s, 5 H), 4.54 (t, 1.7 Hz, 2 H), 4.78 (t, 1.7 Hz, 2 H), 7.27 (t, 8.3 Hz, 1 H), 7.55–7.65 (m, 3 H), 7.80 (d, 8.2 Hz, 2 H), 8.09 (s, 1 H), 8.13 (d, 8.2 Hz, 1 H), 8.21–8.26 (m, 4 H), 9.05 (d, 4.7 Hz, 1 H), 9.21 (s, 1 H). Anal. Calcd for $\text{C}_{39}\text{H}_{24}\text{ClFeN}_2\text{O}_3\text{Re}$: C, 55.36; H, 2.86; N, 3.31. Found: C, 55.58; H, 3.01; N, 3.29.

Structure Determination of 3b. A dark red prismatic crystal of **3b** (dimensions 0.25 \times 0.22 \times 0.12 mm 3) was grown from a dichloromethane solution layered with hexane at room temperature. Crystal, data collection, and refinement parameters are summarized in Table 1. The monoclinic space group C_2 was determined from systematic absences; successful refinement of the structure confirmed the space group assignment. Heavy atom methods were used to locate the Fe atom, while subsequent cycles of least-squares refinements and difference Fourier map were used to locate the remaining non-hydrogen atoms. Hydrogen atoms were placed at calculated positions. All calculations were performed using the SHELX software package.

Table 1. Crystal Data for **3b**

chem formula	$\text{C}_{26}\text{H}_{18}\text{Fe}$
fw	386.25
cryst syst	monoclinic
space group	C_2
<i>a</i> , Å	26.927(6)
<i>b</i> , Å	6.024(2)
<i>c</i> , Å	12.851(2)
β , deg	118.169(2)
<i>V</i> , Å 3	1837.5(7)
<i>Z</i>	4
ρ_{calc} , g/cm 3	1.396
μ , cm $^{-1}$	8.27
$\lambda_{\text{MoK}\alpha}$, Å	0.7107
<i>T</i> , °C	25
total no. of reflns	1779
no. of unique reflns	1174
R^a	0.0529
R_w^b	0.1174
GOF	1.101

$^a R = \{ \sum (|F_o| - |F_c|) / \sum |F_o| \}$. $^b R_w = [\sum w(|F_o| - |F_c|)^2]^{1/2} / \{ \sum w F_o^2 \}$ where $w = (1/\sigma^2)(F_o)$, and the quantity minimized was $\sum w(|F_o| - |F_c|)^2$.

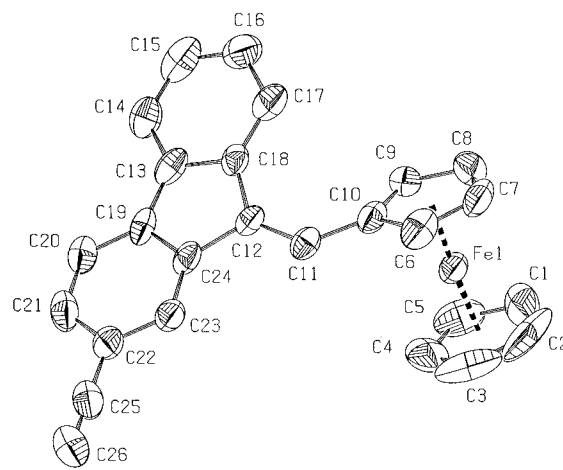
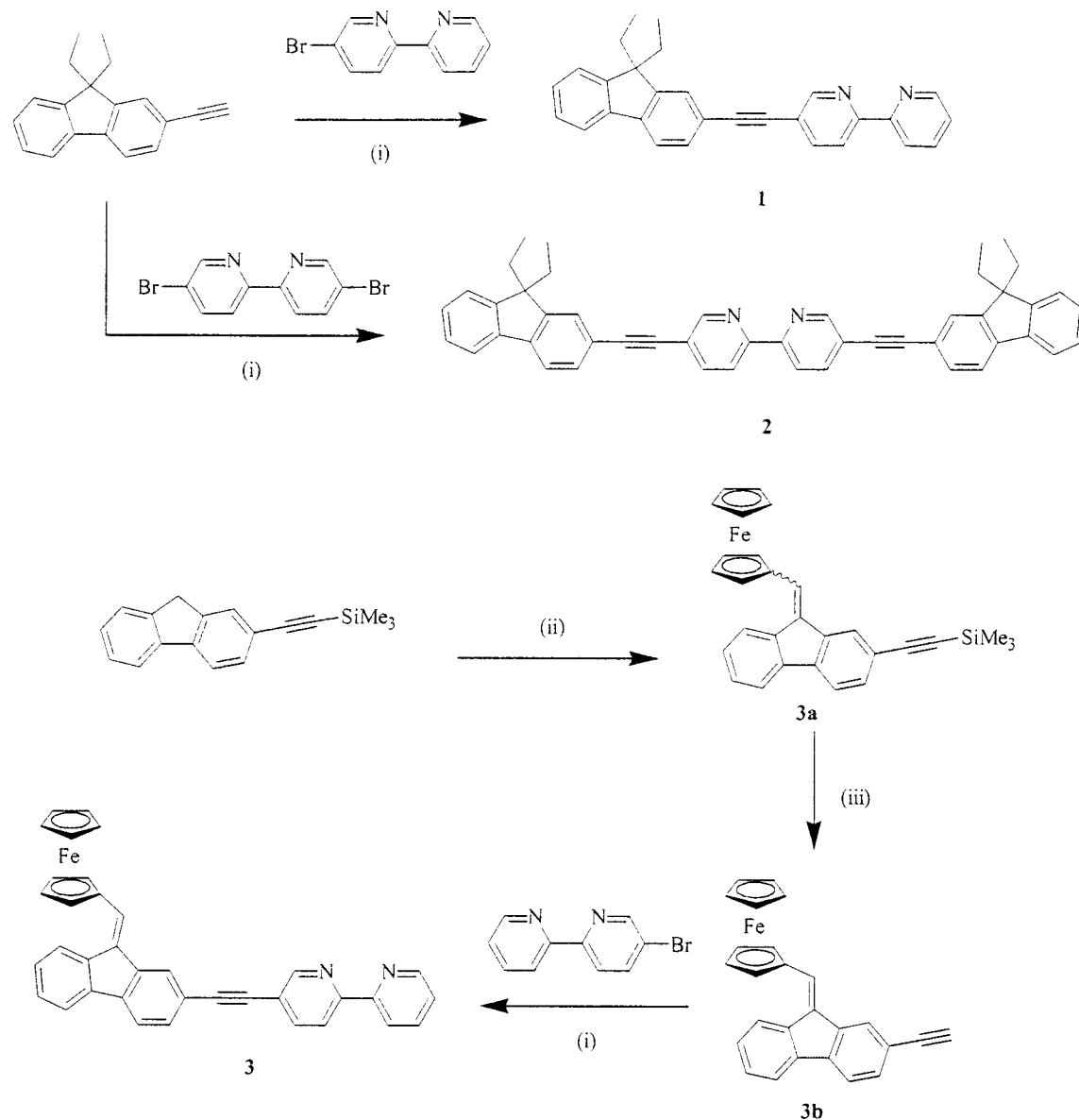


Figure 1. ORTEP diagram of compound **3b**. Hydrogen atoms omitted for clarity.

Results and Discussion

Synthesis, NMR Spectra, and Structure. The syntheses of the polypyridyl ligands were accomplished by the palladium(II)-catalyzed cross-coupling reactions as depicted in Scheme 1. Ferrocene-incorporated terminal acetylene **3b** was prepared by an analogous synthetic route employed earlier for the corresponding diethynyl derivative. 21 In the initial aldol-type condensation both cis and trans isomers were formed. But, careful recrystallization from hexane gave the analytically pure trans isomer. Since the cis isomer was always contaminated with the trans isomer, it was not subjected to further studies. Closer disposition of the ferrocene and bipyridine segments in the cis isomer could probably result in a strongly interacting bimetallic complex. The ligands were characterized by NMR and mass spectra and elemental analysis. The trans orientation of the ferrocene moiety with respect to the ethynyl linkage in **3b** was further confirmed by a single-crystal X-ray diffraction study. The molecular structure of **3b** is displayed in Figure 1. It crystallized in the noncentrosymmetric space group C_2 . The cyclopentadienyl units in the ferrocenyl group assume an eclipsed conformation. The bond lengths and the angles are within

Scheme 1^a

^a (i) Pd(PPh₃)₂Cl₂, PPh₃, CuI, Et₂NH. (ii) *i*-Pr₂NLi, ferrocene carbaldehyde. (iii) MeOH/NaOH, fractional crystallization.

Table 2. Selected Bond Lengths (Å) and Anlgles (deg) in 3b

Fe1–C1 2.01(1)	Fe1–C6 2.017(9)	Fe1–C3 2.018(9)
Fe1–C2 2.02(1)	Fe1–C9 2.030(8)	Fe1–C4 2.03(1)
Fe1–C5 2.04(1)	Fe1–C7 2.04(1)	Fe1–C8 2.041(9)
Fe1–C10 2.060(7)	C25–C26 1.15(1)	
C1–Fe1–C3 66.0(5)	C1–Fe1–C2 37.7(6)	C3–Fe1–C2 40.0(6)
C1–Fe1–C4 66.7(4)	C3–Fe1–C4 39.6(6)	C2–Fe1–C4 66.2(5)
C1–Fe1–C5 40.7(5)	C3–Fe1–C5 66.0(6)	C2–Fe1–C5 65.5(6)
C4–Fe1–C5 38.9(4)	C8–Fe1–C10 68.4(3)	C7–Fe1–C10 68.2(4)
C6–Fe1–C9 68.8(4)	C6–Fe1–C7 40.5(4)	C9–Fe1–C7 68.7(4)
C6–Fe1–C8 68.9(4)	C9–Fe1–C8 40.5(3)	C7–Fe1–C8 41.3(4)
C6–Fe1–C10 40.6(4)	C9–Fe1–C10 40.9(3)	C26–C25–C22 178(2)

the expected range (Table 2). The NMR spectra of the ligands possess features attributable to the bipyridine, fluorene, and ferrocene segments. No anomalous pattern is observed. On complexation with rhenium (Chart 1), a clear downfield shift is observed for the bipyridine protons close to the coordination site, consistent with

that observed for Re(bpy)(CO)₃Cl and related diimine complexes.^{22,23,22,23} In the ruthenium complexes (Chart 1) the signals due to the substituted and unsubstituted bipyridines are overlapping with the peaks arising from the fluorene segment, and so a conclusive assignment is not possible at this stage.

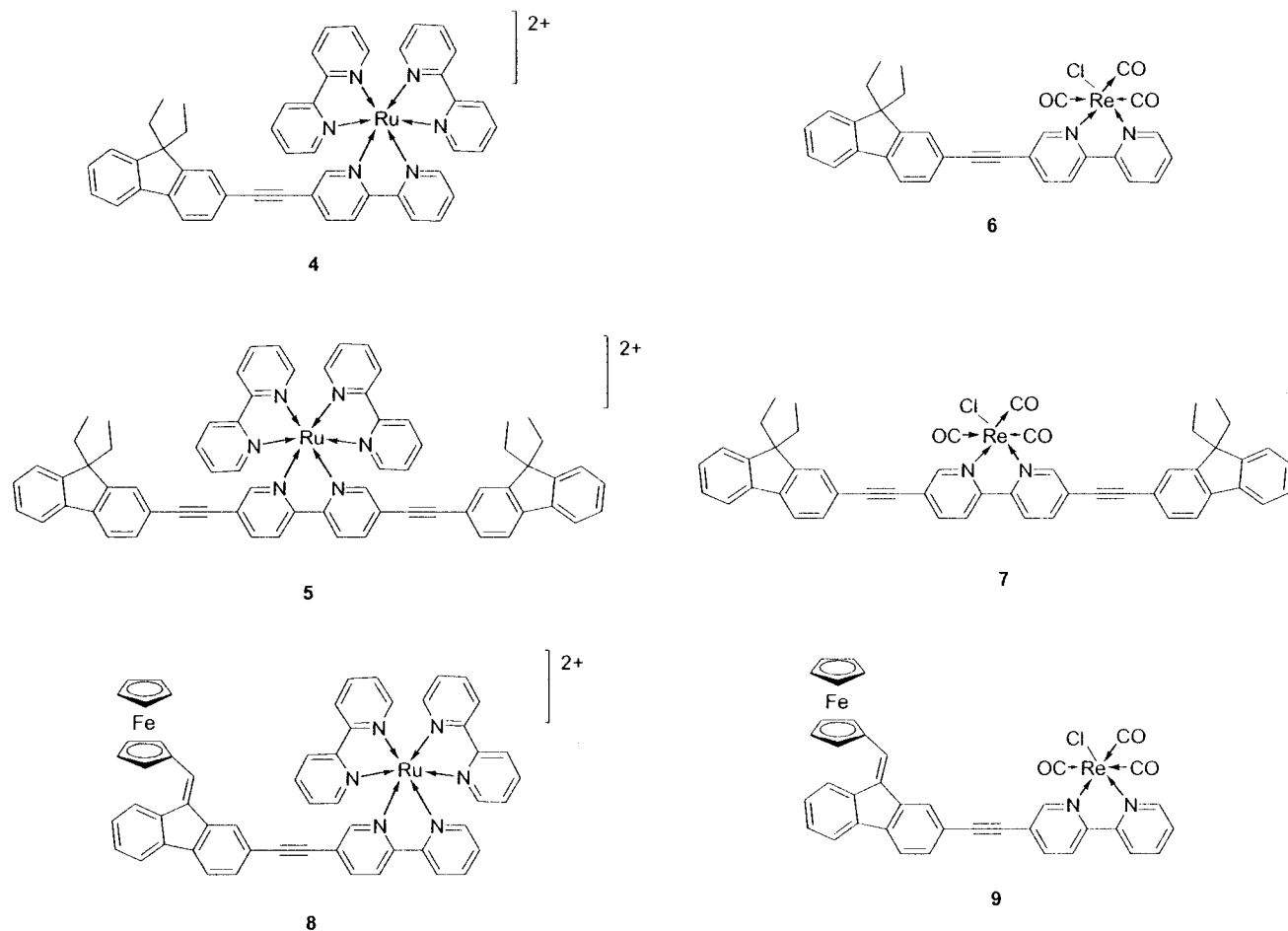
Absorption and Luminescence Properties. The UV–vis absorption data and assignments of Ru(II) complexes reported here along with those of [Ru(bpy)₃]²⁺ and Re(bpy)(CO)₃Cl are listed in Table 3. The assignments of the electronic spectra were made on the basis of the well-documented optical transitions in [Ru(bpy)₃]²⁺ and the related mixed ligand complexes derived from aromatic hydrocarbon linked polypyridyl ligands.^{10–12,24} In general, Ru(II) polypyridyl complexes exhibit two MLCT transitions: the low-energy dπ→π₁* transition and another dπ→π₂* transition located approximately 7000 cm⁻¹ higher in energy. For mixed

(21) (a) Wong, W.-Y.; Wong, W.-K.; Raithby, P. R. *J. Chem. Soc., Dalton Trans.* **1998**, 2761. (b) Wright, M. E.; Cochran, B. B. *Organometallics* **1993**, 12, 3873.

(22) Lees, A. J. *Chem. Rev.* **1987**, 87, 711.

(23) Juris, A.; Campagna, S.; Bidd, I.; Lehn, J.-M.; Ziessel, R. *Inorg. Chem.* **1988**, 27, 4007.

Chart 1

Table 3. Electronic Absorption Spectral Parameters^a

compd	MLCT/d-d	$\pi-\pi^*$ transition
1		343(50.68)
2		369(85.28), 289(25.72)
3b	494(3.86)	340(18.22), 317(25.16), 261(45.18)
3	496(4.51)	342(69.82), 258(38.61)
4	460(sh)	400(29.58), 290(72.56)
5		432(56.08), 321(53.09), 289(76.90)
6		387(29.7), 299(27.34)
7		415(54.36), 319(41.58)
8	460(sh)	388(37.36), 288(89.95)
9	500(4.02)	380(40.98), 318(36.56), 304(37.45), 258(37.19)
Ru(bpy) ₃ ²⁺	451(14.0), 345(6.5), 323(6.5)	285(87.0), 250(25.0), 238(30.0)

^a Recorded in dichloromethane, λ_{\max} in nm and $\epsilon_{\max} \times 10^{-3}$ in $M^{-1} \text{ cm}^{-1}$ in parentheses.

ligand complexes the interpretation of absorption bands is complex, since the lowered symmetry removes the degeneracy of the π^* levels, resulting in the appearance of broad and multiple $d\pi \rightarrow \pi_1^*$ and $d\pi \rightarrow \pi_2^*$ transitions.

The absorption spectra of $[\text{Ru}(\text{bpy})_2(\text{Fbpy})]^{2+}$, $[\text{Ru}(\text{bpy})_2(\text{FcFbpy})]^{2+}$, and $[\text{Ru}(\text{bpy})_2(\text{FcFbpy})]^{2+}$ are shown in Figure 2. They are dominated by the presence of multiple and intense $\pi \rightarrow \pi^*$ transitions arising from the conjugated ligands. In most cases, it is assumed that the $d\pi(\text{M}) \rightarrow \pi^*(\text{bpy})$ transition, if any, is buried under these $\pi \rightarrow \pi^*$ transitions. However, the complexes **4** and **8** possessed a well-resolved shoulder at the low-energy

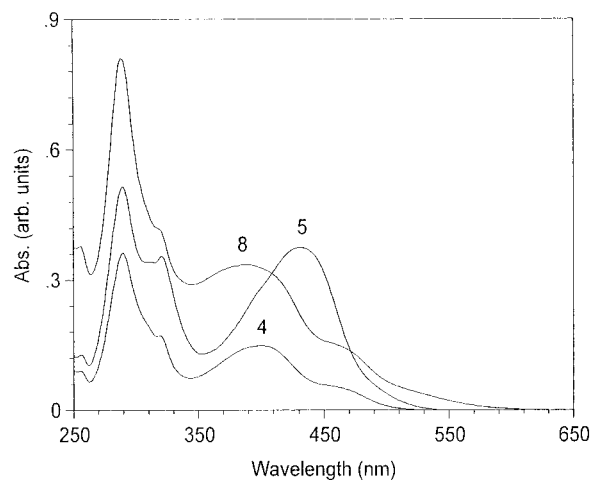


Figure 2. Absorption spectra of the ruthenium complexes **4**, **5**, and **8**.

end, ca. 460 nm, which is tentatively assigned to the $d\pi \rightarrow \pi_1^*(\text{bpy})$ transition in view of its similarity in energy to that observed for $[\text{Ru}(\text{bpy})_3]^{2+}$. When compared to the free ligand, the low-energy $\pi \rightarrow \pi_1^*$ transition in the metal complexes is red-shifted because metalation forces the bipyridyl unit into a planar conformation, thereby effectively increasing the conjugation length.^{24,25}

The absorption spectra of the rhenium(I) complexes consist of two well-resolved bands similar to that of the

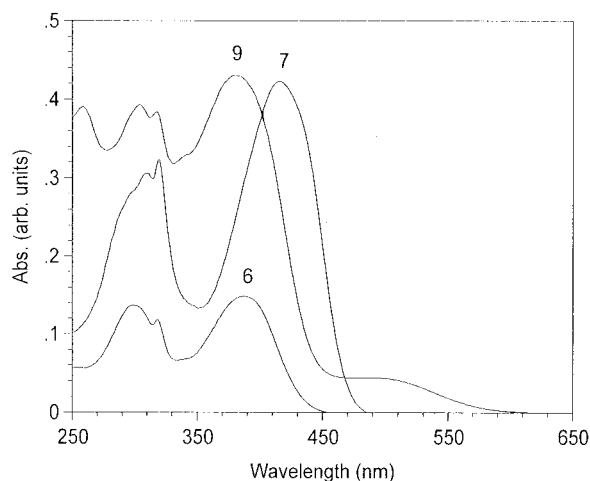


Figure 3. Absorption spectra of the rhenium complexes **6**, **7**, and **9**.

Table 4. Luminescence Parameters for the Compounds^{a,b}

compd	λ_{em} (nm)	ϕ_{em}	τ (ns) ^c
1	413	0.89	1.1
2	433	0.71	0.77
4	623	0.062	1076
5	650	0.058	1187
6	637	0.0021	
7	651	0.0008	
Ru(bpy) ₃ ²⁺	600	0.086	324
Re(bpy)(CO) ₃ Cl	642	0.0031	39

^a λ_{em} = 350 nm (**1**, **2**) or 400 nm (**4**–**7**, Re(bpy)(CO)₃Cl, Ru(bpy)₃²⁺). ^b CH₂Cl₂ (**1**, **2**, **6**, **7**, Re(bpy)(CO)₃Cl) or CH₃CN (**4**, **5**, Ru(bpy)₃²⁺) solution. ^c No reliable lifetime was obtained for **6** and **7** because of their weak emission intensities.

free ligands. However a red shift is noticed for the lower energy absorption of the complexes. These low-energy transitions fall in the order **7** > **6** > **9** (Figure 3). An important point is that the $d\pi(\text{Re}) \rightarrow \pi^*(\text{bpy})$ MLCT transition, which is expected to arise in the 400–500 nm region,²³ is likely buried under the considerably more intense ligand-centered $\pi \rightarrow \pi^*$ transition.

Luminescence was examined in dichloromethane at room temperature, and the parameters are recorded in Table 4. The ligands **1** and **2** exhibited intense blue emission. On the contrary, a weak luminescence was observed for the ruthenium complexes **4** and **5**. Absence of luminescence in **3** and **8** is self-explanatory, as they contain a ferrocene moiety, which is a well-known triplet quencher.²⁶ The fact that **4** and **5** have rather extended lifetimes at room temperature when compared to Ru(bpy)₃²⁺ is of specific interest. Similar but more pronounced enhancement in lifetime was observed for related complexes in which pyrene is covalently linked to bipyridine.¹² Very weak luminescence was also observed for the rhenium(I) complexes **6** and **7**, similar to that recorded for related rhenium(I) diimine complexes. Since no phosphorescence was observed for the ligands,

(24) Wacholtz, W. F.; Auerbach, R. A.; Schmehl, R. H. *Inorg. Chem.* **1986**, 25, 227. (b) Cook, M. J.; Lewis, A. P.; McAuliffe, G. S. G.; Skardy, V.; Thomson, A. J.; Glasper, J. L.; Robbins, D. J. *J. Chem. Soc., Perkin Trans. 2* **1984**, 1293.

(25) Ley, K. D.; Walters, K. A.; Schanze, K. S. *Synth. Met.* **1999**, 102, 1585. (b) Ley, K. D.; Li, Y. T.; Johnson, J. V.; Powell, D. H.; Schanze, K. S. *Chem. Commun.* **1999**, 1749.

(26) Lee, E. J.; Wrighton, M. S. *J. Am. Chem. Soc.* **1991**, 113, 8562.

Table 5. Electrochemical Data^a

compd	ligand reduction	metal oxidation	others
1	−2128(i)		+1563(i)
2	−2152(i), −1924(i)		+1508(i)
3b		+351(87)	
3	−2067(i)	+343(89)	
4	−1350(84), −1725(86)	+1234(76)	+1479(i)
5	−1194(92), −1678(84)	+1292(72)	+1531(i)
6	−1432(87)	+1242(i)	+1666(i), −1794(i)
7	−1288(80)	+1257(i)	+1611(i), −1796(i)
8	−1331(76)	+308(76)	
	−1705(89)	+1290(i)	
9	−1408(77)	+343(84)	−1833(i)

^a Data obtained for dichloromethane solution with sample concentration (10^{−3} M), tetrabutylammonium hexafluorophosphate as electrolyte (0.1 M), scan rate 100 mV/s.

we believe that the origin of emission in these complexes is more likely from a MLCT state.

Electrochemical Properties. Redox potentials for the complexes were determined in dichloromethane by cyclic voltammetry and are tabulated in Table 5. Two reversible reduction waves assigned as bpy-based reductions and a reversible oxidation wave due to the oxidation of ruthenium(II) are observed in complexes **4**, **5**, and **8**. In addition, a ferrocene-based oxidation couple is also located at +0.308 V for **8**. The first reduction wave in these complexes presumably originates from the fluorene-substituted bpy ligand, as high charge density at the second position of fluorene combined with its good π -acid character could stabilize the anion radicals effectively. This assignment is further supported by the fact that bpy reduction potential shifts anodically for the disubstituted derivative, **5**. Ferrocenyl substitution at the ninth position of fluorene has no significant effect on the reduction potential of the bpy ligand, as it does not lie on the effective conjugation pathway. The second reduction wave may be assigned to one of the unsubstituted bpy ligands.

The ruthenium oxidation in complexes **5** and **8** is complicated by the closely following fluorene-based irreversible multielectron oxidation, while a clear reversible wave is seen for **4**. If the switching potential is kept higher than the fluorene oxidation potential, then the reversibility of the ruthenium oxidation is completely disturbed. Similarly, an irreversible oxidation peak at ca. +1250 mV due to the oxidation of Re(I) and an irreversible Re(I) reduction peak at ca. −1800 mV characterize the rhenium complexes. The ferrocene oxidation potentials vary significantly for the ruthenium (**8**) and rhenium (**9**) complexes. The 35 mV cathodic shift observed for the ferrocene oxidation in the ruthenium complex (**8**) may be due to the electronic perturbations caused by the electron-rich ruthenium–bipyridyl segment. On the contrary, a reverse effect may operate in **9** due to the electron-withdrawing rhenium component. Similarly, the anodic shift observed for the ruthenium oxidation in **8** when compared to **4** is a clear manifestation of the destabilizing forces arising due to the ferrocene oxidation.

Conclusion

We have successfully synthesized three fluorene-containing bipyridine ligands, which could serve as models for the polymeric analogues possessing alternat-

ing fluorene and bipyridine units. The bipyridine moieties can be easily linked to a variety of transition metals, as demonstrated in this work for ruthenium and rhenium derivatives. Ferrocene-tethered fluorenyl bipyridine leads to novel heterobimetallic components with rich electrochemistry and serves as a model for polymers possessing redox-active organometallic pendants. We are currently exploring the possibility of extending this methodology to obtain polymeric ligands and their metal complexes that may find use in organic light-emitting diodes.

Acknowledgment. We thank Academia Sinica and the National Science Council (Grant NSC-89-2811-M-001-0066) for financial support.

Supporting Information Available: Tables of atomic coordinates and thermal parameters, all bond distances and angles, and experimental data for X-ray diffraction studies of **3b**. This material is available free of charge via the Internet at <http://pubs.acs.org>.

OM000764N